JOURNAL OF FIRE SCIENCES

Original Article

Journal of Fire Sciences
2017, Vol. 35(1) 36–61

DOI: 10.1177/0734904116679422
journals.sagepub.com/home/jfs
SAGE

Pyrolysis model for a carbon fiber/epoxy structural aerospace composite

Mark B McKinnon[1,2], Yan Ding[2], Stanislav I Stoliarov[2], Sean Crowley[3] and Richard E Lyon[3]

Date received: 5 August 2016; accepted: 25 October 2016

Abstract

Carbon fiber laminate composites have been utilized in the aerospace industry by replacing lightweight aluminum alloy components in the design of aircraft. By replacing low flammability aluminum components by carbon fiber laminates, the potential fuel load for aircraft fires may be increased significantly. A pyrolysis model has been developed for a Toray Co. carbon fiber laminate composite. Development of this model is intended to improve the understanding of the fire response and flammability characteristics of the composite, which complies with Boeing Material Specification 8–276. The work presented here details a methodology used to characterize the composite. The mean error between the predicted curves and the mean experimental mass loss rate curves collected in bench-scale gasification tests was calculated as approximately 17% on average for heat fluxes ranging from 40 to 80 kW m^{-2}. During construction of the model, additional complicating phenomena were investigated. It was shown that the thermal conductivity in the plane of the composite was approximately 15 times larger than the in-depth thermal conductivity, the mass transport was inhibited due to the high density of the laminae in the composite, and oxidation did not appear to significantly affect pyrolysis at heat fluxes up to 60 kW m^{-2}.

Keywords

Carbon fiber composite, fire growth, smoldering, orthotropic properties, mass transport, ThermaKin

[1]Jensen Hughes, Baltimore, MD, USA
[2]Department of Fire Protection Engineering, University of Maryland, College Park, MD, USA
[3]Federal Aviation Administration, William J. Hughes Technical Center, Atlantic City International Airport, Atlantic City, NJ, USA

Corresponding author:
Stanislav I Stoliarov, Department of Fire Protection Engineering, University of Maryland, College Park, MD 20742, USA.
Email: stolia@umd.edu

Introduction

The design of the structure and components as well as the manufacturability of carbon fiber laminate composites has experienced significant improvement in the last few decades, and these improvements have led to increasing prevalence of these composites in a variety of common applications. The aerospace industry has experienced the most widespread adoption of carbon fiber laminates because of the favorable strength-to-weight ratio of these composites compared to metal alloys that have been traditionally used in structural elements in aircraft. In fact, the most recent commercial passenger airplanes from Boeing and Airbus are composed of more than 50% carbon fiber composites by weight and, more notably, the fuselage of the Boeing 787 is completely composed of carbon fiber laminates.[1,2] Some of the advantages that adoption of carbon fiber composites possess over the use of traditional materials include increased fuel efficiency, improved fatigue and corrosion resistance, and the reduction of weight-based maintenance and fees.[3] It has also been noted that minor damage to composite aircraft structures may be easily and quickly repaired.

Though there are numerous advantages to adoption of carbon fiber composites, there are also unavoidable disadvantages that have slowed the replacement of traditional material components with advanced composites. The polymeric matrix materials that are used in laminate composites undergo thermal degradation at elevated temperatures. The fibrous reinforcement materials that compose the laminae can also undergo thermal degradation and oxidation and contribute to the heat released due to the combustion processes that occur in a fire event. As airplane manufacturers seek to benefit from the advantages of carbon fiber laminate composites, fire and associated hazards that contribute to loss of life and property must be taken into consideration.

Historically, fuselage materials have been considered non-flammable and, as such, there is no standard test for the flammability of these materials. Rather, regulations have been designed to prevent penetration of heat, flames, and fire effluent into the cabin. Regulations set by the US Federal Aviation Administration (FAA) focus primarily on post-crash fire scenarios, where loss of life most commonly occurs, and exterior fuel fires caused by fuel spills. A specific concern with post-crash fires is smoldering of carbon fiber structural composites because this form of burning tends to produce more smoke, carbon monoxide, and unburned pyrolysis products than flaming combustion, and smoke inhalation and carbon monoxide poisoning cause the largest percentage of deaths in fires.[4]

It has been estimated that the cost of materials for airplanes is approximately US$300 per pound and production requires large initial investment by the manufacturers.[4] Due to these relatively high costs for airplane cabin materials, it is advantageous for manufacturers in the aerospace industry to completely understand the fire response of materials that may be used to build airplanes before investing in large-scale production. Investigation and improved understanding of the fire response of a material may be facilitated through development and use of a pyrolysis model.

Quintiere et al.[5] conducted an investigation to determine the thermo-physical properties and fire response of the carbon fiber laminate composite that is also the subject of this work. The kinetic and energetic parameters that describe thermal degradation were determined and an analysis of ignition and burning was conducted to better understand the flammability of the material. The thermal conductivity of the composite was measured with an in-house apparatus and the authors ultimately recommended that the measurement be repeated with a more accurate method. The properties that were measured and the observations made during burning experiments provide a data set for comparison with this study. The parameters that accounted for pyrolysis reactions, heat and mass transfer, and material swelling in a thermal

model were determined based on experiments and analysis performed by Quintiere et al.[6] Although the study conducted by Quintiere et al. was extensive, the investigators did not address the possibility of non-one-dimensional heat transfer effects and calculated gas permeability for the material based on assumptions, but did not validate the permeability value against experimental data.

An investigation to characterize carbon fiber composites in fire-like conditions was also conducted by researchers at Sandia National Laboratories[7] that consisted entirely of experimental testing. The investigation involved several configurations of composites that included both epoxy and bismaleimide resin matrix phases and both tape and fabric constructions of carbon fiber laminae. The researchers exposed the samples to radiant heat and conducted piloted ignition flame spread tests and concluded there was no significant difference between tape and fabric constructions, although they were not concerned with developing a pyrolysis model; thus, many of the requisite parameters were not determined. The researchers also concluded that there was no evidence of smoldering in any of the tests, which agrees with conclusions drawn by a more recent study to investigate the fire behavior of carbon fiber/epoxy composites for use in aircraft.[8]

A methodology has been developed to characterize the materials for pyrolysis models that have been successfully demonstrated on non-charring polymers,[9] charring polymers,[10] and composite materials with complicated structures.[11,12] The work presented here consists of an application of this methodology to the carbon fiber composite to parameterize a pyrolysis model that is more accurate than a model based on parameters obtained in previous work.[5] In the process of developing the model, conclusions were drawn regarding mass transport effects and non-isotropic thermal transport due to the complicated structure of the composite and the effect of oxidation on pyrolysis of the composite.

Model

The ThermaKin2D numerical pyrolysis modeling environment was used in this work to conduct inverse analyses on experimental data to indirectly measure thermo-physical properties and reaction parameters to describe the thermal degradation of the carbon fiber composite samples. ThermaKin2D was also used to generate gasification mass loss rate (MLR) and temperature predictions for the sample material to validate the measured properties. ThermaKin2D solves non-steady energy and mass conservation equations accounting for the physical and chemical processes that occur in the condensed phase during pyrolysis.

The sample material is defined geometrically in ThermaKin2D as a series of layers with specified dimensions and chemically and physically as material components described by specific properties. Thermal degradation reactions are accounted for in the model using Arrhenius reaction rate constants. The ThermaKin2D governing equations are provided as equations (1) to (7)

$$\frac{\partial \xi_j}{\partial t} = \sum_{i=1}^{N_r} \nu_i^j r_i - \frac{\partial J_j^x}{\partial x} - \frac{\partial J_j^y}{\partial y} + \frac{\partial}{\partial x}\left(\xi_j \int_0^x \frac{1}{\rho}\frac{\partial \rho}{\partial t} dx\right) \tag{1}$$

$$\sum_{j=1}^{N} \xi_j c_j \frac{\partial T}{\partial t} = -\sum_{i=1}^{N_r} h_i r_i - \frac{\partial q_x}{\partial x} - \frac{\partial q_y}{\partial y} - \frac{\partial I_{ex}}{\partial x} + \frac{\partial I_{rr}}{\partial x} - \sum_{g=1}^{N_g} c_g \left(J_g^x \frac{\partial T}{\partial x} + J_g^y \frac{\partial T}{\partial y}\right) + c\rho \frac{\partial T}{\partial x} \int_0^x \frac{1}{\rho}\frac{\partial \rho}{\partial t} dx \tag{2}$$

$$r_i = A_i \exp\left(\frac{-E_i}{RT}\right)\xi_k\xi_l \tag{3}$$

$$J_g^x = -\rho_g\lambda\frac{\partial(\xi_g/\rho_g)}{\partial x} \tag{4}$$

$$q_x = -k\frac{\partial T}{\partial x} \tag{5}$$

$$\frac{\partial I_{ex}}{\partial x} = -I_{ex}\sum_{j=1}^{N}\kappa_j\xi_j \tag{6}$$

$$\frac{\partial I_{rr}}{\partial x} = \frac{\epsilon\sigma T^4}{I_{ex}^0}\frac{\partial I_{ex}}{\partial x} \tag{7}$$

Equation (1) is the statement for the conservation of mass of component j in terms of the mass concentration of the component, ξ_j ($\mathrm{kg\,m^{-3}}$). The statement for the conservation of mass accounts for consumption or production of component j due to reactions, the rate of which is defined in equation (3), mass transport of gaseous components within the condensed phase which is defined in equation (4), and mass transport associated with contraction or expansion of the material with respect to a stationary boundary ($x = 0$). Equation (2) is a statement for the conservation of energy of the sample in terms of the material temperature, T (K). The statement for the conservation of energy accounts for heat flow due to chemical reactions and phase transitions, heat conduction within the condensed phase, which is defined in equation (5), absorption of radiant heat from external sources defined in equation (6), radiant heat loss from the material to the environment defined in equation (7), convective heat transfer due to gas transport, and energy flow associated with contraction or expansion of the material with respect to a stationary boundary ($x = 0$). No expansion or contraction is allowed in the y-direction.

The symbols in equations (1) to (7) are defined as follows: t (s) denotes time and x and y (m) are the Cartesian coordinates. ρ ($\mathrm{kg\,m^{-3}}$) denotes the density, c ($\mathrm{J\,kg\,K^{-1}}$) is the heat capacity, k ($\mathrm{W\,m^{-1}\,K^{-1}}$) is the thermal conductivity, κ ($\mathrm{m^2\,kg^{-1}}$) is the absorption coefficient, ϵ is the emissivity, and λ ($\mathrm{m^2\,s^{-1}}$) is the mass transport coefficient. All of these thermophysical properties, with the exception of absorption coefficient and emissivity, may be defined as temperature dependent. ν_i^j is the stoichiometric coefficient for component j in reaction i which is positive when the component is produced and negative when the component is consumed. h_i ($\mathrm{J\,kg^{-1}}$) is the heat absorbed or released in each reaction or phase transition and may be defined as temperature dependent. A_i ($(\mathrm{m^3\,kg^{-1}})^{n-1}\,\mathrm{s^{-1}}$) (for reaction of order n) is the Arrhenius pre-exponential factor for reaction i, E_i ($\mathrm{J\,mol^{-1}}$) is the activation energy for reaction i, and R ($\mathrm{J\,mol^{-1}\,K^{-1}}$) is the universal gas constant. I_{ex} ($\mathrm{W\,m^{-2}}$) is defined as the radiation flux from external sources traveling within the material, the superscript 0 in I_{ex}^0 denotes net external radiation flux through the material boundary, and σ ($\mathrm{W\,m^{-2}\,K^{-4}}$) is the Stefan–Boltzmann constant.

The thermo-physical properties appearing without subscripts correspond to the property of a mixture, whereas those with subscripts denote the property of an individual component. The mixture density is calculated as one divided by the sum of the component mass fraction divided by the component density for all components. ThermaKin2D has the ability to

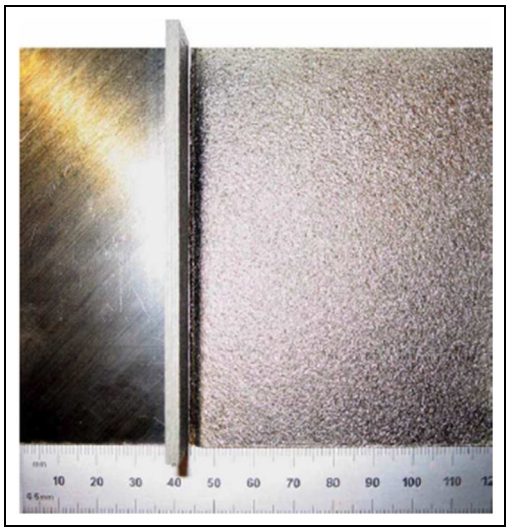

Figure 1. Photograph that includes all surfaces of the Toray Co. BMS 8-276 aerospace composite.[5]

model intumescence by scaling the contribution of gases to the overall volume by a factor related to the local composition. The gases were assumed not to contribute to the volume of the sample in all simulations conducted in this work. Variations in the volume of the composite were modeled by prescribing the densities of condensed phase decomposition products proportional to the stoichiometric coefficients of the products and the overall change in volume as was done in a previous work.[12]

The ThermaKin2D program divides the computational domain into rectangular control volumes (elements) and calculates the temperature and mass of each component in all the elements for each time step. The rate of change of each property is defined as a function of the component masses and element temperature. The resulting coupled algebraic equations are linearized and solved at each time step. A detailed description of the physics represented in the ThermaKin2D modeling environment, the numerical solution approach, and details on the exact form of the mathematical expression for each of the thermo-physical properties are provided elsewhere.[13]

Experiments and analysis

Material

The material studied in this work is a carbon fiber laminate composite produced by Toray Co. in compliance with Boeing Material Specification (BMS) 8-276. The layup is made of 16 plies with an orientation described by $(-45, 0, 45, 90)_{2s}$. This layup features fibers in each successive layer that are rotated 45 degrees with respect to the previous layer and results in a composite that is assumed to possess quasi-isotropic thermal transport properties through the plane of the material. The laminae are composed of continuous carbon fibers and the matrix material is an epoxy resin. The composite is produced in the form of a pre-impregnated panel and is cure toughened at 450 K to satisfy BMS 8-276. Figure 1 displays

the carbon fiber composite samples characterized through this investigation. The density of the composite was measured as 1530 ± 30 kg m^{-3} and the thickness was measured as 3.2 mm. From Figure 1, it is noted that the composite has one face with a smooth surface finish and the other face has a rough surface finish due to the manufacturing process.

Experimental methods

Simultaneous thermal analysis. Simultaneous thermal analysis (STA) is a class of thermal analysis methods that are simultaneously conducted with a single apparatus. In this work, thermogravimetric analysis (TGA) and differential scanning calorimetry (DSC) tests were conducted together with a Netzsch 449 F3 Jupiter STA apparatus to measure the mass and heat flow rate to the sample as a function of temperature and time. The details of calibration of the apparatus and general information on conducting STA tests are available in a previous work.[12]

The temperature program for the STA tests was designed with an initial conditioning period at a constant temperature of 313 K for 20 min followed by heating at a constant set point rate of 10 K min^{-1} to 1100 K (no temperature modulation was used). The test chamber was constantly purged with nitrogen flowing at a rate of 70 mL min^{-1} to investigate the thermal degradation while eliminating oxidation and other unwanted heterogeneous reactions. In all, 10 STA tests were conducted on carbon fiber samples at a set heating rate of 10 K min^{-1}. Three additional STA tests were conducted at a heating rate of 30 K min^{-1} to provide independent *MLR* data for validation of the reaction mechanism determined from data collected at 10 K min^{-1}.

The carbon fiber was cut such that the total mass of the sample ranged from 3 to 10 mg and the layered structure of the laminate was maintained. The prepared sample was placed flat against the bottom of a platinum crucible for the tests. All STA tests were conducted with the crucible lid covering the sample to ensure a uniform temperature profile within the sample. An opening in the center of the lid allowed pyrolyzate gases to escape the crucible as quickly as they were produced.

Inverse analyses were conducted on STA data using a model constructed in ThermaKin2D that adhered to the assumption of infinitely fast transport processes (0D model). Two successive analyses were conducted, first on the *MLR* and total mass data to determine the reaction kinetics to describe the pyrolysis process and second on the heat flow rate data to determine the heat capacity of the composite and heat evolved in each decomposition reaction. The heating rate curves for the STA did not adhere to the set points of 10 and 30 K min^{-1} throughout the tests, and the transient portions of the curves were found to affect modeling of the data in the early test stages. The heating rate was defined to follow its approximate measured temporal evolution in all analyses as described in a previous study.[12]

The inverse analysis to determine the reaction kinetics consisted of identifying an individual mass loss event in the data (reactions) that could be conveniently described by the Arrhenius law, and iterating through combinations of Arrhenius parameters until an adequate agreement was achieved for the event. This process was repeated, starting with the mass loss event that occurred at the lowest temperature and working toward higher temperature events, until the entire *MLR* and total mass curves collected at 10 K min^{-1} were adequately described by the model. The model parameters were independently validated against *MLR* data collected at a heating rate of 30 K min^{-1}. An additional analysis was conducted on the heat flow rate data to determine the heat capacity of the composite and the heat

evolved during each degradation reaction. The heat flow rate data were divided by the instantaneous heating rate to yield an effective heat capacity curve, and linear regression of the curve enabled definition of a temperature-dependent heat capacity. A sensible enthalpy baseline was constructed using a combination of the heat capacity definition and the reaction mechanism. The heat evolved in each reaction was determined as the integral between the heat flow rate curve and the baseline. Further details of these inverse analyses on the STA data are available in a previous work.[12]

Microscale combustion calorimetry. Microscale combustion calorimetry (MCC) is a standard test method[14] in which a mg-sized sample is pyrolyzed in an inert atmosphere under linear heating conditions and the pyrolyzate gases flow to combustion chamber, where the heat release rate (*HRR*) produced as a result of combustion of the pyrolyzate is measured. Three MCC tests were carried out on samples of the carbon fiber composite. The combustor temperature was maintained at 1173 K for all the tests. The crucible was introduced to the pyrolysis chamber and allowed to reach equilibrium at 348 K after which the temperature of the pyrolysis chamber was increased at a set heating rate of 10 K min^{-1} to 900 K. The heats of combustion of the gases produced during thermal degradation of carbon fiber composite samples were determined through an inverse analysis of MCC data in which the *HRR* dependencies on sample temperature were compared to the corresponding *MLR* curves predicted by the kinetic mechanism determined through the analysis of STA data.

A predicted *HRR* curve was generated by simulating the mass loss process in the MCC experiment and applying the heat of combustion value to each distinct gaseous species. The predicted *HRR* curve was compared to the experimental *HRR* curve. Modifications were made to the heat of combustion values until a satisfactory agreement between the predicted and experimental curves was achieved. Further details of this process are available elsewhere.[12]

Gasification experiments and analysis. An apparatus that augments the standard cone calorimeter,[15] the controlled atmosphere pyrolysis apparatus (CAPA),[9,16] was designed to generate well-defined conditions in the vicinity of the sample surface while mass and back surface temperature (T_{back}) data were simultaneously collected. The apparatus features an infrared camera focused on a gold mirror to record a spatially resolved temperature measurement of the back surface of the sample while simultaneously measuring the mass of the sample with the balance internal to the cone calorimeter. The specific details of the design of the CAPA (displayed in Figure 2) are available in previously published related works.[9,12,16]

The majority of the tests conducted in this work with the CAPA had high purity nitrogen (99.998 vol.% N_2) introduced to the gas flow chamber at a flow rate of 225 L min^{-1} (referenced to 1 atm and 298 K). At this flow rate, the mean oxygen concentration approximately 0.001 m from the front surface of the sample was measured as 2.2 ± 0.4 vol.%.[17] This oxygen concentration prevented autoignition for all samples.

CAPA tests were conducted on samples of the carbon fiber composite with both the rough and smooth surfaces subjected to set point heat fluxes of 40, 60, and 80 kW m^{-2} with nitrogen flowing to the CAPA. The number of samples available for this investigation was limited, so two tests were conducted with each surface facing the heater at heat fluxes of 40 and 60 kW m^{-2}, and a single test with each surface facing the heater was conducted at a heat flux of 80 kW m^{-2}. Samples were prepared in a square geometry with a side of 0.08 m

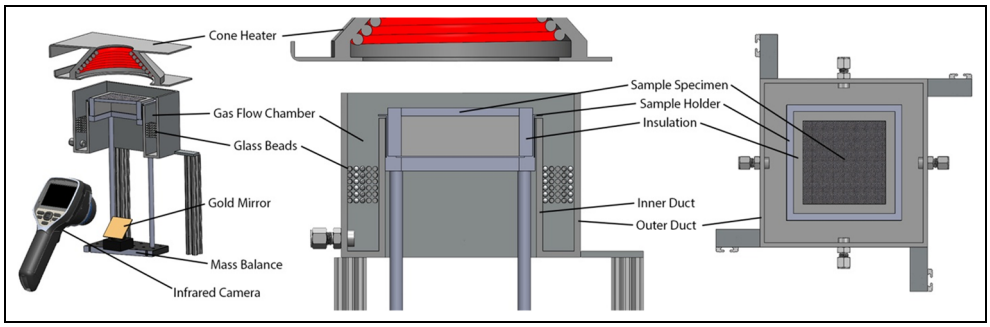

Figure 2. Rendering of the controlled atmosphere pyrolysis apparatus.[12]

and were positioned in the center of a square sheet of 0.00625 m thick Kaowool PM board with an edge dimension of 0.105 m. The back surface of each sample was painted for an emissivity of 0.95 to provide a well-defined surface condition for the infrared camera. The paint was known to partially degrade in the temperature range of approximately 550–650 K, compromising the well-defined emissivity and/or thermal contact, and the data collected above this threshold were considered unreliable and were not used in inverse analyses. The sample and insulation rested on a thin aluminum mesh that provided optical access to the back surface of the sample. Although the back surface of the sample was exposed to air, it was hypothesized that this exposure would not significantly affect the back surface temperature or *MLR* at the sample temperatures generated by the tested heat fluxes. This hypothesis was later confirmed through several tests conducted with various gas atmospheres.

The T_{back} data were recorded at a rate of 7.5 Hz. The mean T_{back} data, which were calculated in each frame according to the sampling method described in a previous work,[12] were generally spatially uniform, with the maximum deviation from the mean value on the order of 5%. Inverse analyses were conducted on the T_{back} data collected in CAPA tests using a one-dimensional (1D) model constructed in ThermaKin2D to determine the parameters that define thermal transport within the composite. The model for the carbon fiber composite was constructed with a single layer under the assumption that the virgin material could be modeled as a homogeneous component with isotropic properties. The mass data collected in CAPA tests did not inform the definition of the thermal transport properties, but served as independent data to validate the model.

Due to the laminate structure of the carbon fiber composites, it was hypothesized that the rate of in-plane heat conduction was larger than in-depth conduction. This hypothesis is consistent with measurements that have been made on carbon fiber/epoxy laminate composites.[18,19] One experiment was conducted to assess the in-plane thermal conductivity relative to the in-depth thermal conductivity in which a sample was irradiated with 40 kW m^{-2} heat flux while half of the surface was covered with 0.0127 m thick Kaowool PM insulation board. A photograph of the prepared sample is provided in Figure 3. The back surface temperatures were monitored throughout the test (using the infrared camera) to enable an inverse modeling of the in-plane thermal transport. The in-plane heat conduction was investigated with a two-dimensional (2D) ThermaKin2D model in which the material and the Kaowool insulation that covered the sample were explicitly modeled. A high conductivity layer was added to the material model to achieve an anisotropic thermal transport within the sample as described in the section "Investigation of in-plane conduction."

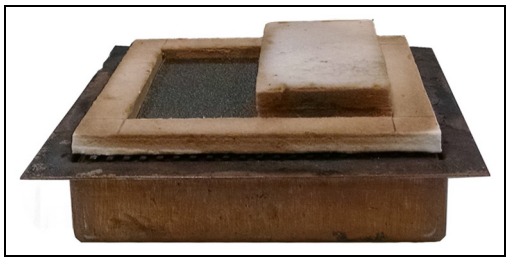

Figure 3. Sample prepared to investigate in-plane heat conduction.

Several tests that utilized a variety of mixtures of nitrogen and oxygen were conducted to investigate the oxidation characteristics of the carbon fiber composite. One test was conducted with a heat flux of 40 kW m^{-2} in which a gas mixture (33.8 L min^{-1} O_2/191.2 L min^{-1} N_2) flowed to the CAPA at a rate of 225 L min^{-1} to generate an oxygen concentration of 15.0 ± 0.5 vol.% approximately 0.001 m from the front surface of the sample (as measured using a Servomex 4100 gas analyzer). This oxygen concentration was chosen to avoid autoignition and flaming combustion of the composite.

Two tests were conducted to elucidate the effect of oxidation on the sample material after the epoxy resin had been degraded. In each test, a sample comprised the material remaining at the end of a test conducted at 60 kW m^{-2} in a nitrogen atmosphere was subjected to a heat flux of 60 kW m^{-2} while 225 L min^{-1} of nitrogen was injected into the CAPA for 600 s followed by 600 s of laboratory air. The oxygen concentration approximately 0.001 m from the front surface of the sample was measured as 20.9 ± 0.5 vol.% when laboratory air was injected in the CAPA. Three type-K thermocouples were inserted in each sample distributed evenly through the thickness of the sample to measure the internal sample temperature throughout the tests. The temperature and *MLR* measurements were made in separate tests to avoid interference between the two measurements.

A 1D model that included the composite material defined with its measured thickness and its back surface exposed to the atmosphere was constructed to aide in analysis of experimental data and to produce predictions of the fire response of the composite. The radiant boundary condition for the front surface was defined with a heat flux identical to the set point for the CAPA tests measured with a water-cooled Schmidt–Boelter heat flux gauge. The convective heat transfer coefficient was defined as 5 W m^{-2} K^{-1} and the ambient temperature for the front surface was measured as 330 K at 30 kW m^{-2} and exhibited a linear dependence on the heat flux set point to 370 K at a heat flux of 70 kW m^{-2}, and this relationship was interpolated and extrapolated the heat fluxes used this work. The mass transport at the front boundary was defined to provide no impedance to the escape of gaseous pyrolyzate produced during degradation. The emissivity of the carbon fiber composite was adopted from the literature,[7] as described in section "Thermal transport parameter determination."

The back surface was defined to be impenetrable to mass transport. The convection coefficient at the back surface of the sample was defined as 4 W m^{-2} K^{-1} with an ambient temperature of 310 K. A radiant heat flux of 0.5 kW m^{-2} was applied to the back surface to simulate radiation from the internal walls of the test apparatus (which were assumed to be at ambient temperature). The back surface was defined to be non-transparent to radiation and its emissivity was defined as 0.95 to simulate the presence of high emissivity paint. A

default value for the mass transport coefficient (2×10^{-5} m^2 s^{-1}) was initially defined for all components.

The convective heat fluxes (representing losses) at the front and back boundaries of the sample were characterized through inverse analyses on data collected in CAPA tests to measure the temperature of a sample-sized copper plate painted for a well-defined emissivity.[16,17] The heat capacity of all gaseous pyrolyzate species was defined as 1800 J kg^{-1} K^{-1}, which was the approximate mean heat capacity of C1–C8 hydrocarbons in the range of 400–500 K.[9] The default value of the mass transport coefficient was found to be high enough to allow all gaseous pyrolyzate to escape the condensed phase with no impedance to flow and low enough that it would maintain the stability of the solution.[20] The mass transport coefficient of all components was modified due to additional analysis after all other properties were determined, as described in the section "Investigation of mass transport effects."

The 2D ThermaKin2D model was constructed with the composite sample defined with its measured thickness and width as well as Kaowool insulation with a thickness of 12.7 mm on the front surface of one half of the composite sample. The Kaowool was assigned thermophysical properties provided by the manufacturer which have been verified in a previous related pyrolysis modeling study.[11] The set point heat flux from the cone heater to the exposed surface of the composite and the insulation were defined in the model as a radiant heat flux boundary condition and all other boundary conditions were defined identical to the 1D model.

The inverse analyses consisted of defining an initial value of the thermal conductivity for the desired components and iteratively modifying the value to improve the agreement between the model prediction and the target temperature data. This process was conducted repeatedly, with the target data selected in increments to encompass the range of time that a specific component comprised the majority of the mass of the sample. Further details of the inverse analysis on the T_{back} data are available in a previous work.[12] The thermal transport parameters for the composite that were determined through analysis using the 1D model were unchanged in the 2D model.

Results

Data analysis for property evaluation

Thermal degradation kinetics and energetics determination. It was assumed that the reaction mechanism that described thermal degradation of the carbon fiber composite consisted completely of consecutive reactions because only the epoxy resin underwent degradation. Although there was only a single distinct peak in the TGA *MLR* curve, its complicated shape combined with a complex shape of the DSC heat flow rate curve necessitated several additional reactions. The derived reaction mechanism is summarized in Table 1 and the experimental and simulated mass loss curves corresponding to the decomposition of the composite are plotted in Figure 4. In Figure 4, the sample mass (m) and the *MLR* are normalized by the initial mass (m_0). Throughout this work, error bars are defined as two standard deviations of the mean.

The components defined in the reaction mechanism for pyrolysis models are generally not chemically distinct species, but in fact a mixture of distinct species that may be conveniently completely or partially isolated to facilitate characterization of thermo-physical properties. In this work, the subscript virgin corresponds to the initial unreacted material component.

Table 1. Effective reaction mechanism for carbon fiber composite and the heats of reactions.

#	Reaction equation	A $((m^3\ kg^{-1})^{n-1}s^{-1})$	E $(J\ mol^{-1})$	h $(J\ kg^{-1})$
1	$Composite_{virgin} \rightarrow 0.989Composite_{int1} + 0.011Composite_{vol1}$	4.09×10^5	$9.1\,8 \times 10^4$	-1.8×10^4
2	$Composite_{int1} \rightarrow 0.902Composite_{int2} + 0.098Composite_{vol2}$	6.16×10^{19}	2.78×10^5	-3.8×10^4
3	$Composite_{int2} \rightarrow 0.911Composite_{int3} + 0.089Composite_{vol3}$	1.23×10^{21}	3.01×10^5	1.8×10^4
4	$0.5Composite_{int3} + 0.5Composite_{int4} \rightarrow 0.888Composite_{residue} + 0.112Composite_{vol4}$	8.00×10^5	1.50×10^5	1.0×10^4

Positive heats represent endothermic processes (absorbed energy during the reaction).

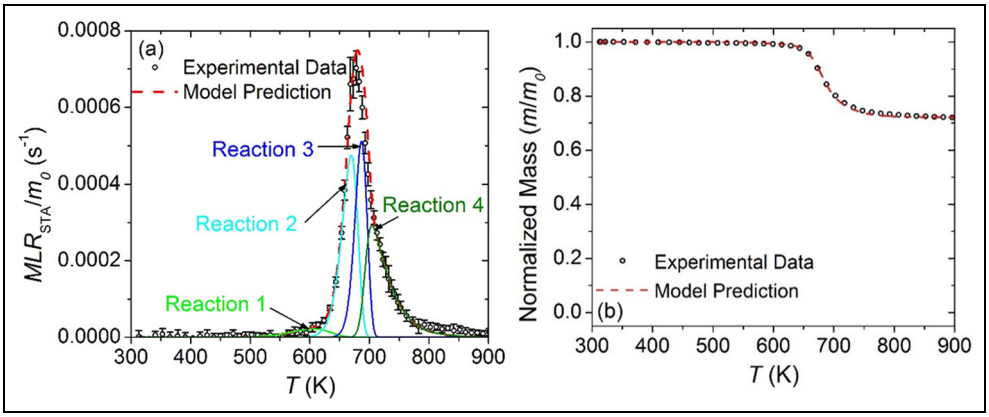

Figure 4. (a) Normalized mass loss rate and (b) normalized mass data collected in 10 K min^{-1} STA experiments and model-predicted curves for the carbon fiber composite.

The solid products of degradation may be the final products, referred to here as the residual component ($Composite_{residue}$), or may be intermediate products that eventually degrade to the final products, referred to here with the subscript int followed by a number that corresponds to the reaction that forms the intermediate component. The $Composite_{residue}$ component defined in the model corresponds to a state of the physical sample that is composed primarily of undegraded carbon fibers with a minor contribution from the char formed from degradation of the epoxy resin. The subscript vol refers to the gaseous pyrolyzate products formed during degradation, and the number in the subscript corresponds to the reaction which forms the volatile product.

Initially, a three-reaction mechanism was identified to adequately represent the *MLR* data. Upon examination of the heat flow rate data from the STA tests, it was determined

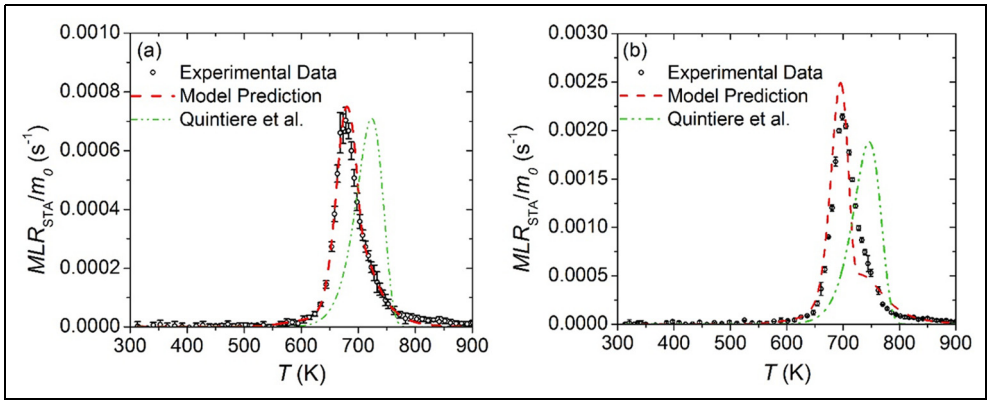

Figure 5. Experimental normalized mass loss rate plotted with predictions from this work and Quintiere et al.[5] for set heating rates of (a) 10 K min^{-1} and (b) 30 K min^{-1}.

that an additional reaction was required to describe the shape of the heat flow rate curve. This four-reaction mechanism was found to adequately represent the thermo-gravimetric and energetic response of the carbon fiber composite through thermal degradation. It was determined that the mechanism provided the best representation of the mass loss process when all reactions were defined as first-order reactions and the final reaction was defined as a second-order reaction. The mean relative error between the experimental *MLR* curve and the curve predicted with the kinetic mechanism defined in Table 1 was approximately 7%, which was within the scatter of the measurements. The mean relative error between the experimental and predicted normalized mass curves was approximately 0.4%.

Each kinetic parameter was varied independently while maintaining the mean relative error within the mean scatter of the experimental data to determine the uncertainty in the parameters determined through the inverse analysis procedure used in this work. The uncertainty in the pre-exponential factor was determined as $\pm 20\%$ and the uncertainty in the activation energy was calculated as $\pm 1\%$. Note that these uncertainties correspond to independent variation of each parameter and they do not take into account potential interdependence of these parameters.

MLR predictions made with the model parameterized in this chapter and a previous study on the carbon fiber composite conducted by Quintiere et al.[5] are compared to experimental data in Figure 5. A single-step, first-order reaction mechanism was defined by Quintiere et al. of which the kinetic parameters were determined through analysis of TGA data collected at four heating rates. Figure 5(a) displays both predicted curves and the experimental data from this work at a set heating rate of 10 K min^{-1} and Figure 5(b) shows the predictions and experimental data at a heating rate of 30 K min^{-1}.

The curves predicted by Quintiere et al. capture the qualitative shape of the experimental data at both heating rates, although the temperature at which the maximum *MLR* occurs in each case is over-predicted by approximately 50 K. The maximum experimental *MLR* was captured at 10 K min^{-1} by the model produced by Quintiere et al., although the maximum *MLR* measured at 30 K min^{-1} was under-predicted by approximately 10%. The disagreement between the model produced by Quintiere et al. and the model produced in this work is

Table 2. Heat capacity values for each solid component in the carbon fiber composite.

Component	c (J kg^{-1} K^{-1})	Source
$Composite_{virgin}$	$160 + 2.4T$	STA
$Composite_{int1}$	1415	Interpolated
$Composite_{int2}$	1470	Interpolated
$Composite_{int3}$	1525	Interpolated
$Composite_{residue}$	$1054 + 0.7T$	Butland and Maddison[21]

likely the result of the method used to determine the kinetics of the degradation process and variations between the calibrations of the instruments used in each study.

The heat capacity of each component defined in the reaction mechanism is provided in Table 2. A linear temperature-dependent relationship was found to provide the best representation of the heat capacity of the $Composite_{virgin}$ component from data collected in STA tests. The residual mass that remained at temperatures above approximately 800 K was characterized by a porous structure that compromised the thermal contact between the sample and the crucible and yielded unreliable heat flow rate measurements. This was exemplified by a rapid increase in the heat flow rate from 800 K to approximately 1100 K that did not correspond to a physically realistic process. This unreliable heat flow rate data at high temperatures led to adoption of a literature value for the heat capacity of the residual component. The $Composite_{residue}$ component was assigned a linear, temperature-dependent heat capacity that was calculated from a least-squares linear regression conducted by Butland and Maddison[21] on a survey of data for the heat capacity of graphite.

The intermediate components that were produced and consumed during thermal degradation of the composite could not be isolated for direct measurement of the heat capacity. The heat capacities of $Composite_{int1}$, $Composite_{int2}$, and $Composite_{int3}$ were defined as a linear combination of the heat capacity defined for the $Composite_{virgin}$ and $Composite_{residue}$ components evaluated between 500 and 750 K. The heat capacity of the $Composite_{int2}$ component was defined as the mean of the heat capacities of $Composite_{virgin}$ evaluated at 500 K and $Composite_{residue}$ evaluated at 750 K. The heat capacity of $Composite_{int1}$ was defined as the mean of the heat capacity of $Composite_{virgin}$ evaluated at 500 K and the heat capacity of $Composite_{int2}$. The heat capacity of $Composite_{int3}$ was defined as the mean of the heat capacity of $Composite_{residue}$ evaluated at 750 K and the heat capacity of $Composite_{int2}$.

The heat flow rate data collected in the STA tests is plotted in Figure 6 along with the sensible enthalpy baseline constructed from the heat capacities from Table 2 and component masses modeled by the mechanism provided in Table 1. The experimental curve features local minima at 515 and 663 K and a maximum at approximately 690 K. It is clear from Figure 6 that the experimental heat flow rate curve is below the sensible enthalpy baseline curve between 500 and 680 K and the maximum that occurs at 690 K is above the baseline. Although the entire process of thermal degradation of the carbon fiber composite is endothermic (positive heat flow rates), there are exothermic reactions that contribute to its thermal degradation.

A heat of reaction (displayed in Table 1) was assigned to each reaction to match the experimental heat flow rate curve. The analysis yielded exothermic heats of reaction for the first and second reactions and endothermic heats for the last two reactions. Exothermic

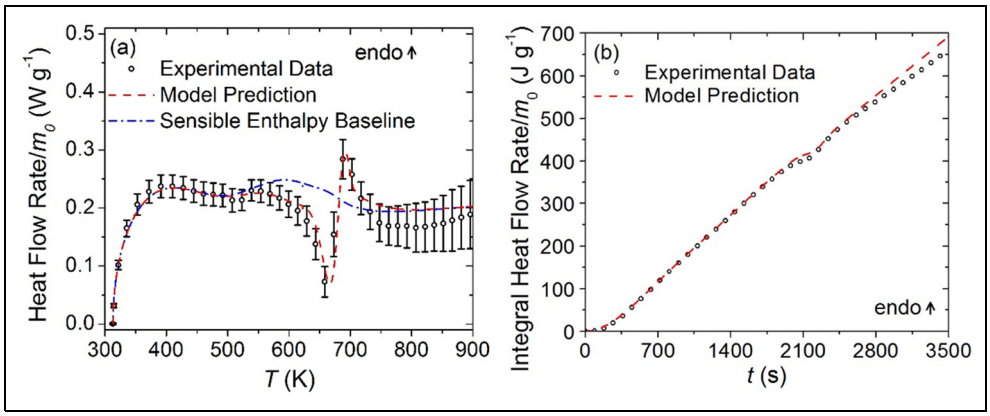

Figure 6. (a) Normalized heat flow rate and (b) integral heat flow rate data collected in STA experiments and model-predicted curves for carbon fiber composite.

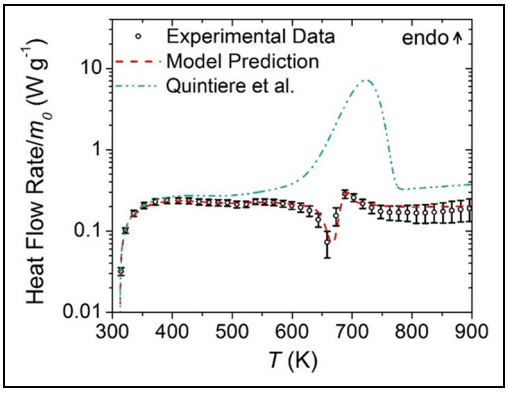

Figure 7. Normalized heat flow rate measured and predicted in this study as well as the prediction based on the data from Quintiere et al.[5]

decomposition reactions are unusual but were observed previously for charring polymers and explained by Li and Stoliarov.[22]

The uncertainty in the heat capacity of virgin and melt components was determined as ±10% by varying the heat capacity definition to generate a heat flow rate curve prediction that was within the scatter of the experimental data. The method used to determine the heats of reaction yielded heats of reaction with uncertainties of approximately ±20%.

The heat absorbed during the thermal degradation reaction defined by Quintiere et al.[5] was considerably larger (more endothermic) than the heat evolved in all of the reactions defined in the current investigation. The heat flow rate curve predicted in the current investigation and the curve predicted from the parameters determined in the investigation conducted by Quintiere et al. are plotted in Figure 7 with the experimental heat flow rate data. The overall heat of degradation determined by Quintiere et al. is approximately an order of

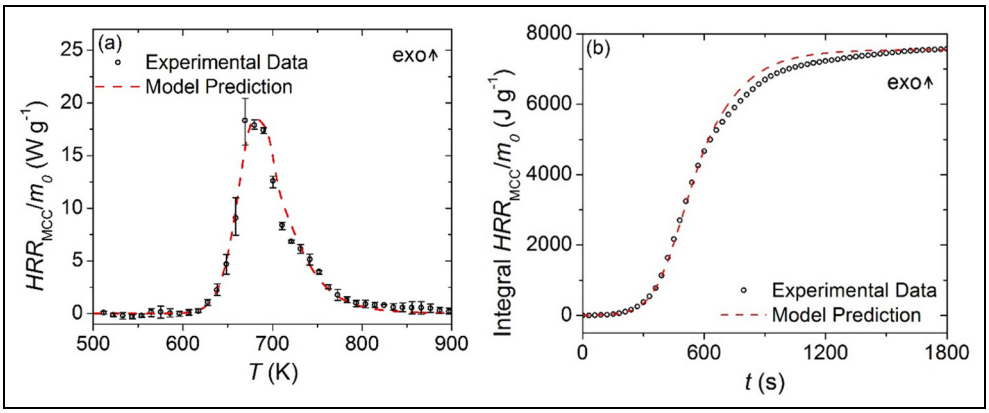

Figure 8. (a) Normalized heat release rate and (b) integral heat release rate data collected in MCC experiments and model-predicted curves for the carbon fiber composite.

Table 3. Effective heat of combustion values for the volatile species released in each reaction.

Volatile species	h_c (J kg^{-1})
$Composite_{vol1}$	0
$Composite_{vol2}$	2.4×10^7
$Composite_{vol3}$	2.3×10^7
$Composite_{vol4}$	3.7×10^7

Positive heats of combustion are exothermic.

magnitude larger than that determined in this work, while the sensible enthalpy curves are similar at relatively low temperatures. It is possible that the disagreement between the heat of reaction values measured in these two studies is related to the type of DSC apparatus utilized for each. It has been noted[23] that the heats of polymer decomposition are more accurately determined with the apparatus used in this investigation, a heat flux DSC apparatus, than with a power-compensation type DSC used by Quintiere et al.

Heat of combustion determination. The experimental and predicted *HRR* curves and integral *HRR* curves are provided in Figure 8. The aggregate heat of combustion (h_c) determined in this investigation was calculated from these data as 2.7×10^7 J kg^{-1} of volatiles, compared to the value measured by Quintiere et al.[5] which was 2.65×10^7 J kg^{-1} of volatiles. These values are within the uncertainty associated with reproducibility of measurements made with the MCC apparatus (6%).

The mass loss associated with the first thermal degradation reaction corresponded to a zero magnitude heat release and the heat of combustion was defined as zero to maintain agreement between the experimental and simulated *HRR* curves. The heats of combustion of the products of the three remaining thermal degradation reactions were determined as non-zero values that are displayed in Table 3. Contrary to the convention used to define the heats of reaction, positive values in Table 3 correspond to exothermic processes.

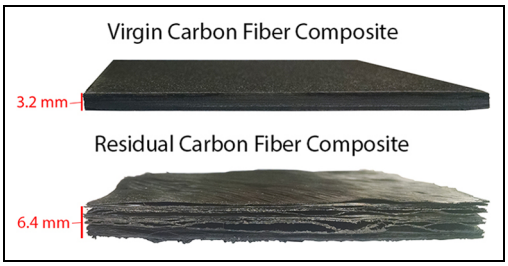

Figure 9. Comparison of the thickness of the virgin carbon fiber composite to the residual composite after cooling from a radiant heating gasification test at 60 kW m^{-2}.

Thermal transport parameter determination. The thermal conductivity of all of the components defined in this pyrolysis model for the carbon fiber composite was determined through an inverse analysis procedure conducted on the data collected in bench-scale gasification tests with a heat flux of 40 kW m^{-2}. The inverse analysis required that the emissivity and absorption coefficient was defined for each component. The emissivity of the carbon fiber composite was not directly measured in this work, although the emissivity of several different carbon fiber composites has been measured by researchers at Sandia National Laboratories.[7] The near-normal emissivity was measured in the Sandia study as 0.86 for the smooth surface and 0.90 for the rough surface of a carbon fiber composite similar to the material studied here. By comparing the experimental data that were collected with the rough surface and the smooth surface facing the heater, it was determined that the difference in surface finish did not significantly affect the T_{back} or MLR data. The emissivity values measured by Sandia were within the range of emissivity values measured for carbon composites in a more recent study,[24] which further justified adoption of this literature value. In an effort to simplify the model, the emissivity of the $Composite_{virgin}$ component, as well as all the $Composite_{int}$ components, was defined as 0.86.

The structural stability of the composite eliminated the possibility of separating the individual layers to facilitate the direct measurement of the absorption coefficient with a method utilized in a previous work.[12] The laminae were composed of continuous carbon fibers and were clearly non-transparent to either visible or near infrared light. To make the simulations consistent with this observation, the absorption coefficient of all components was defined to ensure no significant radiation was allowed to transmit through the sample (100 m^2 kg^{-1}). The emissivity of graphite was measured at elevated temperatures as approximately 0.86[25] and was defined as the emissivity of the $Composite_{residue}$ component. This value has been used to describe the emissivity of char components in several previous related studies.[11,12] These assumptions led to definition of all components in the model with an absorption coefficient of 100 m^2 kg^{-1} and an emissivity of 0.86.

The thickness of the carbon fiber composite sample was observed to increase in gasification tests as individual layers partially delaminated from the composite. This increase in thickness occurred gradually over the course of the test, and the observation of this increase is consistent with observations made in previous work conducted on carbon fiber composites.[5–7] Although there was scatter in the measured increase in thickness, the measurements have been approximated for this model as an increase of 100% of the original thickness of the sample regardless of the radiant heat flux, which resulted in a sample that was

Table 4. Thermo-physical properties for the condensed phase components defined in the carbon fiber composite pyrolysis model.

Component	ρ (kg m^{-3})	k (W m^{-1} K^{-1})	ϵ	κ (m^2 kg^{-1})
$\text{Composite}_{\text{virgin}}$	1520	$0.59–0.00065T$	0.86	100
$\text{Composite}_{\text{int1}}$	1203	$0.295–0.000325T + 2.75 \times 10^{-10}T^3$	0.86	100
$\text{Composite}_{\text{int2}}$	905	$0.295–0.000325T + 2.75 \times 10^{-10}T^3$	0.86	100
$\text{Composite}_{\text{int3}}$	706	$0.295–0.000325T + 2.75 \times 10^{-10}T^3$	0.86	100
$\text{Composite}_{\text{residue}}$	549	$5.5 \times 10^{-10}T^3$	0.86	100

approximately 6.4 mm thick at the end of the simulated gasification. Figure 9 shows the photographs of the composite prior to and after testing to emphasize the change in thickness.

The density of the $\text{Composite}_{\text{virgin}}$ component was defined equal to the measured density of the composite, and the density of each subsequent component was defined to decrease systematically from the density of the reactant that decomposed to form that component to simulate the observed increase in the thickness of the sample. The thickness was defined to increase by 25% over the course of each reaction. The product density was decreased from the reactant density by a factor equal to the stoichiometric coefficient for the solid product of degradation for the reaction divided by the factor by which the thickness increased, for example, the density for $\text{Composite}_{\text{int1}}$ was calculated as (1521 kg m^{-3}) (0.989/1.25). The definitions for the densities and optical properties of all components are provided in Table 4.

The mean T_{back} data collected in four CAPA tests at 40 kW m^{-2} with the smooth surface and the rough surface facing the heater are presented in Figure 10. The T_{back} increased rapidly to approximately 550 K, where the temperature remained relatively constant for a short period, after which the T_{back} continued to rise slowly to a steady temperature of approximately 600 K. Observations of the experiments led to the conclusion that the period of almost constant temperature at 550 K corresponded to degradation or de-bonding of the high emissivity paint on the back surface of the sample.

The initial rise of the T_{back} data curve was chosen as the target for the inverse analysis conducted to determine the thermal conductivity of the $\text{Composite}_{\text{virgin}}$ component because this was the only component that affected the T_{back} curve early in the tests. The temperature prediction was not sensitive to the thermal transport parameters of the residual and intermediate components up to 120 s in Figure 10 and all components were defined with the same thermal conductivity for this portion of the analysis.

A similar inverse analysis was conducted to determine the thermal conductivity of the $\text{Composite}_{\text{residue}}$. The target data for the inverse analysis were chosen as the portion of the T_{back} curve that was collected after 120 s into the gasification tests, as indicated in Figure 10. Although these data were considered to be somewhat unreliable (due to onset of decomposition of the high emissivity coating), they represented the best data set from which to characterize the thermal conductivity of the residual component. Due to the high porosity and temperature of the carbonaceous residual mass, radiation was assumed to be the dominant mode of heat transfer through the sample when $\text{Composite}_{\text{residue}}$ was the major component. The radiation diffusion approximation[26] was invoked to describe the thermal conductivity of the residual component with an expression of the form βT^3, where β is a user-defined

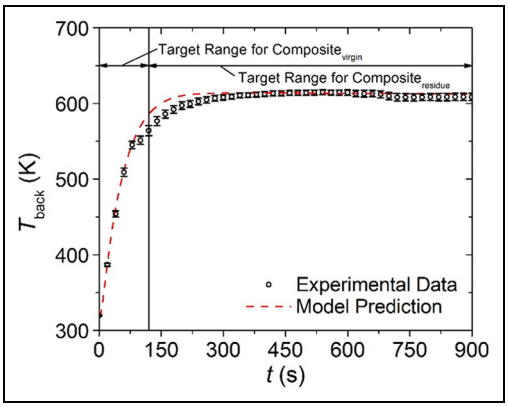

Figure 10. Experimental back surface temperature history measured in CAPA tests and corresponding model-predicted curve for the carbon fiber composite exposed to a radiant flux of 40 kW m^{-2}.

constant. Throughout this inverse analysis, the thermal conductivities of all the intermediate components were defined as the mean of the thermal conductivity of $Composite_{virgin}$ and $Composite_{residue}$. The uncertainties in the thermal conductivities were estimated to be ±15%. The full set of parameters that were determined for the composite to describe thermal transport to and within the solid sample are provided in Tables 2 and 4.

Model validation and further analysis

Predictions of the T_{back} and MLR of the carbon fiber composite from the fully parameterized pyrolysis model are plotted against the experimental data in Figure 11. Note that only STA data and the T_{back} data collected in CAPA tests at 40 kW m^{-2} were used to determine parameters for this model. Consequently, the MLR prediction at 40 kW m^{-2} and the T_{back} and MLR predictions at 60 and 80 kW m^{-2} are compared to experimental data for independent validation of the model parameters.

The rise in temperature up to the 550 K threshold was highly repeatable at all temperatures and was well predicted by the model developed in this work at 40 and 60 kW m^{-2}. The slope of the initial rise in T_{back} predicted at 80 kW m^{-2} was well predicted, although the time to the onset of temperature rise was slightly over-predicted. The experimental MLR data collected at all heat fluxes are characterized by a single distinct peak as well as a local maximum/inflection point approximately 60–180 s after the peak. The MLR data gradually decreased to zero following the inflection point in the data. All of the MLR predictions from the model developed in this work made with the default mass transport definition ($\lambda = 2.0 \times 10^{-5}$ m^2 s^{-1}) captured the rising edge of the experimental curve. The time to the peak of the experimental curve was well predicted at 40 kW m^{-2} and over-predicted by greater margins with increasing heat flux. The qualitative shape of each curve predicted in this work did not agree with the corresponding experimental curve. The curves predicted at each heat flux tended to over-predict the magnitude of the peak of the experimental curve as well as the data collected between the peak and the subsequent inflection point. The curves generated by the model in this work tended to under-predict the magnitude of the MLR curve from the inflection point until the end of the test.

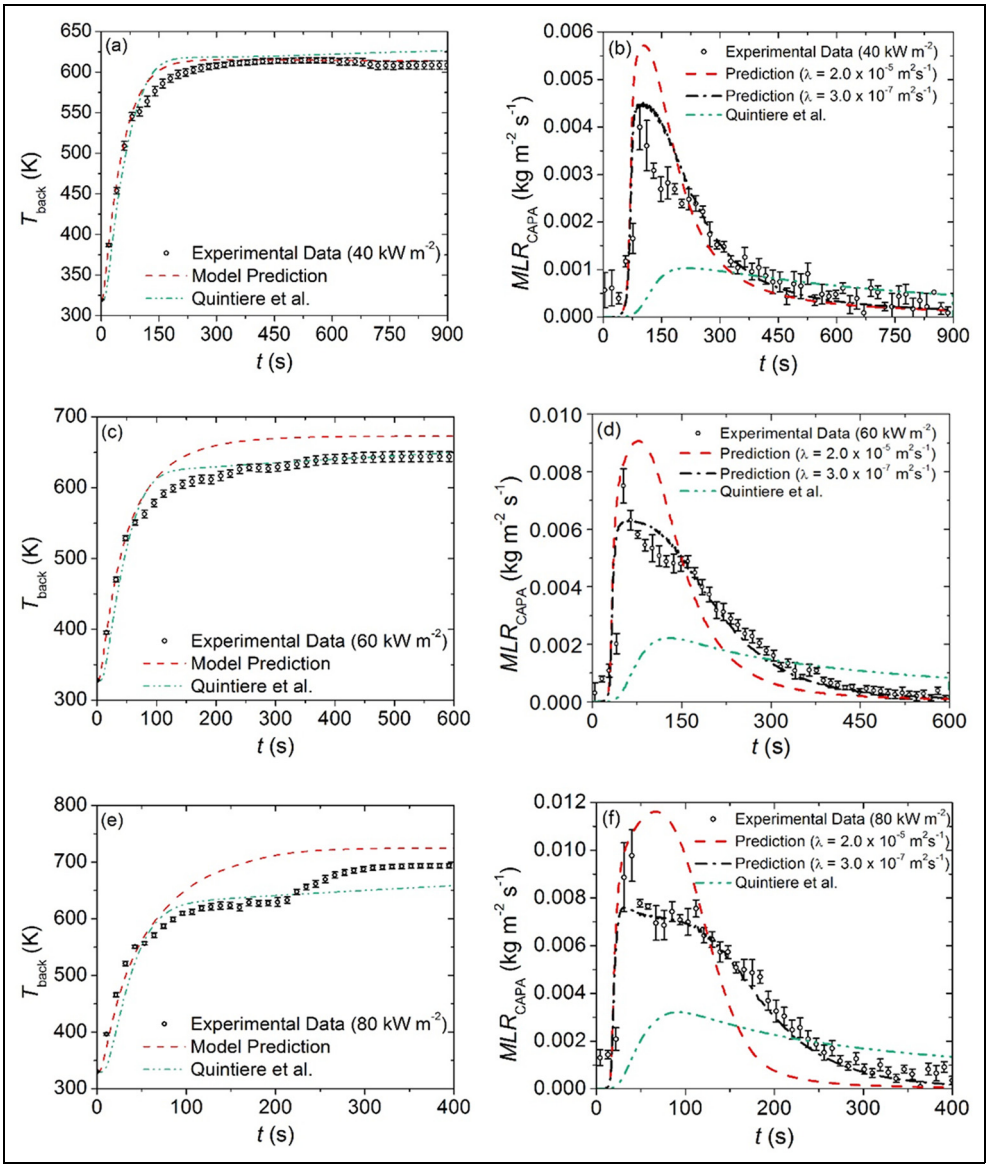

Figure 11. Model-predicted and experimental T_{back} and *MLR* data collected in CAPA tests at incident heat fluxes of (a, b) 40 kW m^{-2}, (c, d) 60 kW m^{-2}, and (e, f) 80 kW m^{-2}.

Figure 11 also includes the predictions from the model parameterized with the property values determined by Quintiere et al.[5] The T_{back} profile predicted by the model parameterized with the values determined by Quintiere et al. has a slightly worse agreement than the model parameterized in this work at 40 kW m^{-2} and a better agreement at the higher heat fluxes. These agreements are misleading because the data collected above 600 K are expected

to be systematically lower than the actual T_{back} due to the compromised coating, and the model based on the properties measured by Quintiere et al. tends to under-predict these data. Furthermore, the *MLR* curves are not well predicted using the property set measured by Quintiere et al. This poor prediction is primarily associated with the heat of the degradation reaction, which is too high.

Investigation of mass transport effects. It is clear in the plots provided in Figure 11 that the *MLR* predictions from the model defined with the default mass transport coefficient did not capture the shape of the experimental curve, and it was hypothesized that the discrepancies between the model predictions and experimental data were caused by inhibited mass transport within the composite. Whereas the pyrolysis of common polymers is characterized by the entire irradiated surface releasing pyrolyzate gas, the gasification of the carbon fiber composite featured few localized points on the surface where pyrolyzate gas escaped from the solid. This observation indicated that the high density of the laminae in the composite contributed to mass transport effects. Reduced mass transport effects have also been observed in highly cross-linked polymers[27] like the epoxy resin used to construct the composite studied in this work. The effect of a reduced mass transport coefficient on the measured *MLR* was verified during modeling by adjusting the mass transport coefficient from the default value of 2.0×10^{-5} m^2 s^{-1} downward to a value of 3.0×10^{-7} m^2 s^{-1} to account for resistance to the free flow of pyrolyzate within the sample. The *MLR* curves predicted by the model parameterized with the lower mass transport coefficient are plotted in Figure 11. The temperature predictions were unaffected by the adjusted mass transport coefficient.

The qualitative shape of the tail of the experimental *MLR* curves in Figure 11 was well predicted by the modified model at each heat flux. The time to the peak *MLR* was represented by the model at all heat fluxes, although the magnitude of the peak was underpredicted for the 60 and 80 kW m^{-2} cases. The overall agreement between the model predictions and the experimental data was improved with the lower mass transport coefficient. The mean instantaneous error between the predicted curve and the experimental curve for all heat fluxes was approximately 17%.

It was hypothesized that the pressure in the composite would increase with a reduction in the free flow of pyrolyzate through the material, and to assess the feasibility of this reduced mass transport coefficient, an estimation of the internal pressure due to gas buildup in the composite during pyrolysis was performed using the gas concentrations calculated with ThermaKin2D. According to the simulation, the maximum pyrolyzate gas concentration found in the sample with the reduced transport coefficient was approximately 28 kg m^{-3} at a temperature of 670 K. The mean molar mass of the gaseous species produced during pyrolysis of epoxy resin and similar polymers is approximately 0.28 kg mol^{-1}.[28–30] The maximum pressure estimated through a crude calculation using the ideal gas law was about 6×10^5 Pa. Measurements of the internal pressures in glass-fiber-reinforced polymer composites have been as high as 1×10^6 Pa (10 atm)[31] and the tensile strength of the Toray composite tested in this work has been measured as 2.7×10^9 Pa[32] at room temperature, although it may be as low as 1.3×10^9 Pa at 670 K and 1.4×10^8 Pa at 980 K.[33] These data indicate that the mass transport coefficient is reasonable because the pressure increase associated with lower mass transport rates is similar to pressures measured in the past and two orders of magnitude lower than the tensile strength of the composite. This calculation

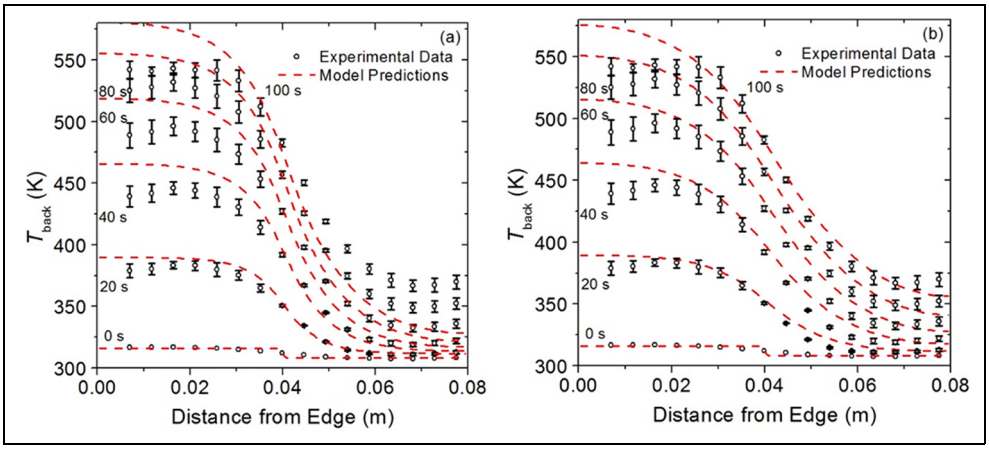

Figure 12. Experimental data and model predictions of temperature distribution across the back surface of the sample partially covered with thermal insulation at various times after onset of 40 kW m^{-2} radiant exposure (a) with single thermal conductivity definition and (b) with additional high conductivity layer.

indicates that the composite is likely to maintain its structural integrity in the presence of such pressure, which is consistent with observations of gasification tests of the composite.

Investigation of in-plane conduction. It was hypothesized that the thermal conductivity values presented in the section "Thermal transport parameter determination" were appropriate to describe in-depth heat conduction and inappropriate for in-plane heat conduction. Simulation data from the 2D model with an unmodified thermal conductivity are provided in Figure 12(a) with experimental data. Each data point represents the mean value from four points across the back surface of the sample (parallel to the edge of the insulation on the sample surface). These data points were collected at 16 locations perpendicular to the edge of the insulation (each location is classified according to its distance from the edge of the sample that was not covered by insulation). It is apparent from Figure 12(a) that the isotropic thermal conductivity definition for the composite is inaccurate.

An additional low-density ($\rho = 100$ kg m^{-3}), low-heat capacity ($c = 100$ J kg^{-1} K^{-1}), high thermal conductivity, non-reacting layer approximately 10% the thickness of the sample was introduced to the geometric center of the sample. The thermal conductivity of the additional layer was adjusted as part of an inverse analysis on the back temperature data to determine the rate of heat conduction in the plane of the material relative to the conduction into the depth of the sample. The inverse analysis yielded a thermal conductivity of 50 W m^{-1} K^{-1} of the additional thin layer introduced to the model and the resulting model-predicted curves are provided in Figure 12(b). Although the agreement between the model prediction and the experimental data is not perfect, the prediction provides a reasonable estimate for the in-plane thermal conductivity of the composite. Deviations between the prediction and the experimental data at the edges (0 and 0.08 m from the edge) may be caused by the modeling assumption of adiabatic boundaries, when, in fact, the insulation at the boundaries allows some heat diffusion. Using the well-known expression for the conductivity of materials layered in parallel to the direction of heat flow,[34] the thermal conductivity

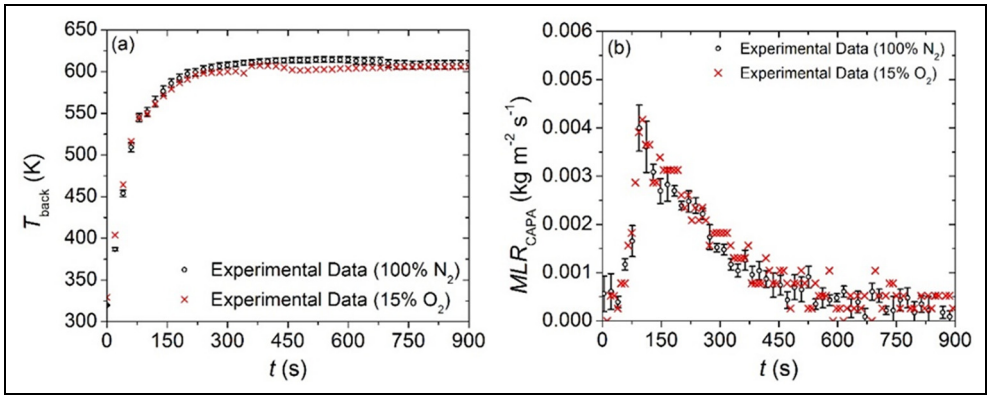

Figure 13. (a) Back surface temperature and (b) *MLR* curves for the carbon fiber composite irradiated with 40 kW m^{-2} of heat flux in nitrogen and 15 vol.% O_2 (balance N_2) atmospheres.

of the mixture may be calculated. The in-plane thermal conductivity of the carbon fiber composite was calculated as 4.8 W m^{-1} K^{-1}. This value appears to be reasonable because the literature values for the in-plane thermal conductivity for carbon fiber composites range from 10 to 15 times larger than the in-depth thermal conductivity,[18,19] and the ratio between the in-plane and the in-depth thermal conductivity determined here is about 15.

A 1D simulation was conducted with the additional highly conductive layer to identify the effect of the layer on in-depth conduction. The layer was defined with a mass transport coefficient of 2.0×10^{-5} m^2 s^{-1} to ensure that it did not introduce any unphysical resistance to the flow of pyrolyzate gases to the model. The T_{back} and MLR profiles produced by the 1D model were identical with and without the highly conductive layer, which confirmed that the presence of this additional layer did not affect in-depth conduction or mass transport.

Investigation of oxidation. The results of tests conducted to determine the effects of oxidation on the pyrolysis of the carbon fiber composite are presented in Figures 13 and 14. Since the reinforcement in the composite was made of carbon fibers, the composite was potentially highly susceptible to oxidation at high temperatures due to large surface area of these fibers. Thus, it was hypothesized that the presence of oxygen may affect the MLR and T_{back} histories. The T_{back} and MLR curves collected in 15 vol.% of oxygen (balance nitrogen) and the mean data collected in nitrogen (2.2 vol.% of O_2) at the same external heat flux are displayed in Figure 13. The uncertainties in the T_{back} data are not shown to avoid congestion. It is evident from the figure that the addition of oxygen to the gasification test on the undegraded sample did not significantly change the temperature or the MLR history at 40 kW m^{-2}.

An attempt was made to determine the oxidation kinetics of the carbon fiber from the experimental data collected on residual mass samples that were tested in nitrogen and air at 60 kW m^{-2}, although it was ultimately concluded that oxidation had only a subtle effect on the pyrolysis process. The temperature and mass data are displayed in Figure 14. The three different sets of data points in Figure 14(a) each correspond to one of the thermocouples and variations between these data sets are due to the distance from the surface of the sample to each thermocouple.

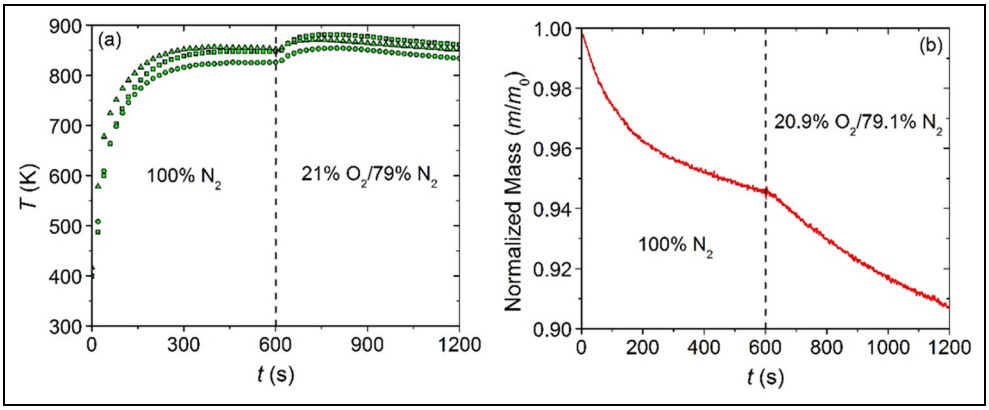

Figure 14. (a) Internal temperatures and (b) normalized mass measured for the carbon fiber composite residue samples irradiated with 60 kW m^{-2} of heat flux in tests with 600 s of nitrogen followed by 600 s of air atmosphere.

The plot in Figure 14(b) shows that the residual mass sample continued to lose mass at a slow rate over the first 600 s of the test. This mass loss may be attributed to further degradation of residual resin as well as, to a minor degree, evaporation of moisture. When the oxygen content of the atmosphere was increased after 600 s, a change in the pyrolysis process occurred which manifested as a sample temperature increase and a more rapid decrease in the sample mass. The increase in the MLR is due to oxidation reaction and the increase in the temperature is caused by exothermicity of this reaction. These increases were relatively small and it was concluded from these data that the oxidation rate was not sufficiently high to support a hypothesis that the residual carbon fiber may undergo a self-sustained oxidation (or smoldering) in the absence of a strong external heat source. This result is consistent with observations made during radiant heating tests[7] and impinging flame tests[8] on carbon fiber composite samples. The study conducted by Sandia[7] concluded that the carbon fiber surface temperature must be in excess of approximately 1173 K for significant oxidation to occur.

Conclusion

A complete set of thermo-physical properties and reaction parameters were determined for a carbon fiber aerospace composite through a systematic methodology. STA tests were conducted on samples of the composite and the resulting data were analyzed to determine the parameters that define thermal degradation reactions and the heat capacity for all identified components. The reaction mechanism was developed from *MLR* and heat flow rate data collected at a set point heating rate of 10 K min^{-1} and independently validated against *MLR* data obtained at 30 K min^{-1}. Analysis of MCC data provided the heats of combustion for the volatile species produced in each thermal degradation reaction and further verified this reaction mechanism.

Multiple bench-scale gasification tests at a wide range of external heat fluxes were conducted on the composite with the CAPA in which the back surface temperature (T_{back}) and

MLR data were collected. Inverse analyses on the T_{back} data allowed the extraction of thermal transport parameters for the composite. There did not appear to be a difference imposed on the collected data due to whether the smooth or textured face of the composite was facing the heater during the gasification tests. All of the parameters that defined the model were validated against data collected outside the calibration conditions.

Resistance to mass transport within the sample was observed due to the structure of the carbon fiber reinforcement and the highly cross-linked epoxy resin which was accounted for by reducing the mass transport coefficient for all components to 3.0×10^{-7} m^2 s^{-1}. By modifying the mass transport coefficient, the agreement between the model prediction and experimental data improved significantly. It appears that the possibility of this reduced mass transport must be considered when studying the pyrolysis of densely packed laminates.

The in-plane thermal conductivity was evaluated by analyzing data from a test with partially obstructed radiant flux to the front surface of the sample using the 2D formulation of ThermaKin2D. It was determined that the in-plane thermal conductivity was approximately 15 times larger than the in-depth thermal conductivity in the temperature range of 300–600 K. This conclusion indicates that orthotropic properties must be accounted for when attempting to model fire growth on carbon fiber–reinforced composites. Additional CAPA tests were conducted to investigate the effect of oxygen in the atmosphere on the pyrolysis process. A 15 vol.% oxygen atmosphere had no effect on the data collected at 40 kW m^{-2}. Data collected on residual mass samples when subjected to a 21 vol.% oxygen atmosphere yielded only small variations from the data collected in nitrogen. These data lead to the conclusions that smoldering of the composite is not likely to occur in any state, and the rate of oxidation is insignificant at the temperatures produced by 60 kW m^{-2} imposed radiant heat flux.

Declaration of conflicting interests

The author(s) declared no potential conflicts of interest with respect to the research, authorship, and/or publication of this article.

Funding

This work was supported by the Federal Aviation Administration Grant #12-G-011.

References

1. Boeing. Boeing: 787 Dreamliner, http://www.boeing.com/commercial/787/#/design-highlights/visionary-design/composites/advanced-composite-use/ (2015accessed 2 January 2016).
2. AIRBUS. AIRBUS passenger aircraft—A350 XWB, A350 XWB Fam, http://www.airbus.com/aircraftfamilies/passengeraircraft/a350xwbfamily/ (2016accessed 20 October 2016).
3. Mouritz AP. *Fire safety of advanced composites for aircraft B2004/0046*, 2006, https://www.atsb.gov.au/media/32739/grant_20040046.pdf
4. Lyon RE. Fire-resistant materials: research overview. Final report, Federal Aviation Administration, Atlantic City, NJ, December 1997.
5. Quintiere JG, Walters RN and Crowley S. *Flammability properties of aircraft carbon-fiber structural composite*. Technical report, Report no. DOT/FAA/AR-07/57, October 2007, pp. 8–72, https://www.fire.tc.faa.gov/pdf/07-57.pdf
6. McGurn MT, DesJardin PE and Dodd AB. Numerical simulation of expansion and charring of carbon-epoxy laminates in fire environments. *Int J Heat Mass Tran* 2012; 55: 272–281.
7. Hubbard JA, Brown AL, Dodd AB, et al. *Carbon fiber composite characterization in adverse thermal environments*. SANDIA report, Report no. SAND2011-2833, May 2011, http://prod.sandia.gov/techlib/access-control.cgi/2011/112833.pdf
8. Tranchard P, Samyn F, Duquesne S, et al. Fire behaviour of carbon fibre epoxy composite for aircraft: novel test bench and experimental study. *J Fire Sci* 2015; 33: 247–266.
9. Li J, Gong J and Stoliarov SI. Gasification experiments for pyrolysis model parameterization and validation. *Int J Heat Mass Tran* 2014; 77: 738–744.
10. Li J, Gong J and Stoliarov SI. Development of pyrolysis models for charring polymers. *Polym Degrad Stabil* 2015; 115: 138–152.

11. McKinnon MB, Stoliarov SI and Witkowski A. Development of a pyrolysis model for corrugated cardboard. *Combust Flame* 2013; 160: 2595–2607.
12. McKinnon M and Stoliarov S. Pyrolysis model development for a multilayer floor covering. *Materials* 2015; 8: 6117–6153.
13. Stoliarov SI, Leventon IT and Lyon RE. Two-dimensional model of burning for pyrolyzable solids. *Fire Mater* 2014; 38: 391–408.
14. ASTM D7309:2013. Standard test method for determining flammability characteristics of plastics and other solid materials using microscale combustion.
15. ASTM E1354:2015. Standard test method for heat and visible smoke release rates for materials and products using an oxygen consumption calorimeter.
16. Semmes MR, Liu X, McKinnon MB, et al. A model for oxidative pyrolysis of corrugated cardboard. In: van Hees P, Jansson R and Nilsson D (eds) *Proceedings of the 11th international symposium international association for fire safety science*, Canterbury, New Zealand, 10–14 February 2014. International Association of Fire Safety Science.
17. Li J. *A multiscale approach to parameterization of burning models for polymeric materials*. MS Thesis, University of Maryland, College Park, MD, 2014.
18. Tian T and Cole KD. Anisotropic thermal conductivity measurement of carbon-fiber/epoxy composite materials. *Int J Heat Mass Tran* 2012; 55: 6530–6537.
19. Dowding KJ, Beck JV and Blackwell BF. Estimation of directional-dependent thermal properties in a carbon-carbon composite. *Int J Heat Mass Tran* 1996; 39: 3157–3164.
20. Stoliarov SI, Crowley S, Lyon RE, et al. Prediction of the burning rates of non-charring polymers. *Combust Flame* 2009; 156: 1068–1083.
21. Butland ATD and Maddison RJ. The specific heat of graphite: an evaluation of measurements. *J Nucl Mater* 1973; 49: 45–56.
22. Li J and Stoliarov SI. Measurement of kinetics and thermodynamics of the thermal degradation for charring polymers. *Polym Degrad Stabil* 2014; 106: 2–15.
23. Stoliarov SI and Li J. Parameterization and validation of pyrolysis models for polymeric materials. *Fire Technol* 2016; 52: 79–91.
24. Boulet P, Brissinger D, Collin A, et al. On the influence of the sample absorptivity when studying the thermal degradation of materials. *Materials* 2015; 8: 5398–5413.
25. Matsumoto T and Ono A. Specific heat capacity and emissivity measurements of ribbon-shaped graphite using pulse current heating. *Int J Thermophys* 1995; 16: 267–275.
26. Siegel R and Howell J. *Thermal radiation heat transfer*. New York: Taylor & Francis, 2002.
27. Buchanan AC and Britt PF. Investigations of restricted mass transport effects on hydrocarbon pyrolysis mechanisms through silica immobilization. *J Anal Appl Pyrol* 2000; 54: 127–151.
28. Matsubara H and Ohtani H. Evaluation of molecular weight of original epoxy acrylates in UV-cured resins by pyrolysis-gas chromatography in the presence of organic alkali. *J Anal Appl Pyrol* 2006; 75: 226–235.
29. Balabanovich AI. GC/MS identification of pyrolysis products from fire-retardant brominated epoxy resin. *J Fire Sci* 2005; 23: 227–245.
30. Galipo RC, Egan WJ, Aust JF, et al. Pyrolysis gas chromatography/mass spectrometry investigation of a thermally cured polymer. *J Anal Appl Pyrol* 1998; 45: 23–40.
31. Hariharan R, Test FL, Florio J, et al. Internal pressure and temperature distribution in decomposing polymer composites. In: Hetsroni G (ed.) *Proceedings of the ninth international heat transfer conference*, Jerusalem, Israel, 19–24 August 1990, pp. 335–340. New York: Hemisphere Pub. Corp.
32. Connell JW. An overview of thermoplastic structural composites for aerospace applications. In: *Proceedings of the international conference on high performance plastic*, Vienna, 5–6 April 2005, p. 178. Akron: Smithers Rapra Publishing.
33. Wang K, Young B and Smith ST. Mechanical properties of pultruded carbon fibre-reinforced polymer (CFRP) plates at elevated temperatures. *Eng Struct* 2011; 33: 2154–2161.
34. Holman JP. *Heat transfer*. 7th ed. New York: McGraw-Hill, 1990.

Author biographies

Mark B McKinnon is an associate at Jensen Hughes in Baltimore, MD, USA. Dr McKinnon holds an MS in Fire Protection Engineering and a PhD in Mechanical Engineering.

Yan Ding is a PhD candidate in the Mechanical Engineering Department at the University of Maryland, College Park, USA.

Stanislav I Stoliarov is an associate professor at the Fire Protection Engineering Department of the University of Maryland, College Park, USA. Dr Stoliarov holds MS in Chemical Engineering and PhD in Physical Chemistry. His research interests include polymer flammability, pyrolysis and smoldering mechanisms, and flame structure and spread.

Sean Crowley is a senior technician working at the Federal Aviation Administration's William J. Hughes Technical Center at the Atlantic City International Airport, New Jersey, USA.

Richard E Lyon is manager of Fire Research at the Federal Aviation Administration's William J. Hughes Technical Center at the Atlantic City International Airport in New Jersey, USA, a position he has held since 1993. Prior to that, Dr Lyon worked as a research engineer for 8 years in the Chemistry and Materials Science Department at Lawrence Livermore National Laboratory, Livermore, California.